Evaluation of Deep Subsurface Resistivity Imaging for Hydrofracture Monitoring

Project Number: DE-FE0013902

Second Quarterly Progress Report
Project Period: Oct. 1, 2013 – Sept. 30, 2015
Period Covered: Jan. 1, 2014 – March 31, 2014

for
U. S. Department of Energy
National Energy Technology Laboratory

Principal Investigator: Dr. Andrew D. Hibbs
858.381.4146, ahibbs@groundmetrics.com

Submitting Official: Gayle Guy
858.381.4147, gguy@groundmetrics.com

GroundMetrics, Inc.
4217 Ponderosa Ave, Suite A
San Diego, CA 92123
DUNS: 968252382

Other team members: Berkeley Geophysics Associates, Global Microseismic Services

April 30, 2014

Signed: _____
Gayle Guy, Corporate Communications Manager
For Dr. Andrew Hibbs

1 Disclaimer

This report was prepared as an account of work sponsored by an agency of the United States Government. Neither the United States Government nor any agency thereof, nor any of their employees, makes any warranty, express or implied, or assumes any legal liability or responsibility for the accuracy, completeness, or usefulness of any information, apparatus, product, or process disclosed, or represents that its use would not infringe privately owned rights. Reference herein to any specific commercial product, process, or service by trade name, trademark, manufacturer, or otherwise does not necessarily constitute or imply its endorsement, recommendation, or favoring by the United States Government or any agency thereof. The views and opinions of authors expressed herein do not necessarily state or reflect those of the United States Government or any agency thereof.

2 Table of Contents

Contents

3 Executive Summary

Hydraulic fracturing (fracking) has enabled commercial production from unconventional formations. However, fracking is more expensive than the conventional methods used to produce gas and oil, and fracked wells exhibit a much faster decline in production than conventional wells. Furthermore there are environmental concerns with the amount of water that is needed, pollution of groundwater reservoirs, triggering earthquakes, and the release of methane into the atmosphere. A key concern of the general public is hydrofracturing out of the formation and into the groundwater table.

Unconventional wells exhibit highly variable production in a given area and often the majority of gas or oil produced comes from only a few of the fracturing stages. As a result more extensive fracturing operations are performed than are really needed, resulting in excess proppant being pumped into the formation. These inefficiencies indicate that the eventual destination of the injected fluids used in reservoir stimulation is poorly understood.

The objective of this project is to quantify how well an in-situ measurement of bulk electrical resistivity using the new method of Depth to Surface Electromagnetic (DSEM) imaging can be related to the changes in rock properties and fluid propagation that occur as a result of hydraulic fracturing. Electromagnetic data will be processed to quantify the EM signal and compared with simultaneously acquired microseismic data to establish both the benefit of the EM data alone and combining them with microseismic data.

This report covers the second quarter of the 24-month project. During this reporting period, we successfully ran our 3D code, ordered and received multiple pieces of sensing hardware and were accepted for presentations at four different industry conferences.

4 Accomplishments

4.1 Milestone Log

	Planned	Actual
Project Management Plan	**10/2013**	**10/2013**

Status: Complete

M1. Completion of Code	**01/31/2014**	**3/20/14***
Status: To be completed January 31, 2014.		
M2. Assembly of Sensor & Receiver Hardware	**03/30/2014**	**3/15/14**
Status: To be completed March 30, 2014.		
M3. Completion of DSEM and Seismic Survey	**8/15/2014**	
Status: To be completed August 15, 2014.		
M4. Identify Change in the DSEM Data Due to Fracking	**8/31/2014**	
Status: To be completed August 31, 2014.		
M5. Invert Data to Produce a 3D Subsurface Image	**9/30/2014**	
Status: To be completed September 30, 2014.		
M6. Quantify Resistivity Change Due to Fracking	**3/31/2015**	
Status: To be completed March 31, 2015.		
M7. Define Clear Case for EM to Improve Hydrofracking	**9/30/2015**	
Status: To be completed September 30, 2015.		

*M1 was nominally complete on time in that the code was delivered by 1/31/14 but troubleshooting/bug fixes have delayed its full implementation. It is now running efficiently.

4.2 Project Description

The specific problem addressed in this project is to quantify whether a measurement of resistivity can provide improved monitoring of SRV during fracking. DSEM provides the first capability to image resistivity in deep hydrocarbon reservoirs with horizontal completion. This comes down to two subsidiary problems: A) whether a sufficient EM signal exists when acquired via DSEM, and B) whether the EM data can be effectively combined with seismic data to significantly improve imaging and quantification of SRV. This project will experimentally address problem A. For problem B we will investigate three basic avenues to combine EM and TFI information using the data collected to address problem A.

The following work was completed in this reporting period.

4.3 Work Completed

4.3.1 Task 2 - Model DSEM Signal of a Fracture Network

The goal of this task is to estimate the range of surface electric fields for a typical fracture network. There are two basic steps: a) project the change in rock resistivity as a result of hydrofractures. We assume that the fracturing fluid is more conductive than the host rock and forms a connected conducting anomaly. The calculation will be of the reduction in resistivity (= increase in conductivity), and b) project the change in electric field at the surface due to the change in rock resistivity resulting from hydrofracturing.

4.3.1.1 Task 2.1 Project the change in electrical resistivity due to hydrofractures

As discussed in our first report our initial approach is to calculate the fracture signal via adapting a prior published model.[1] In this prior model a fracture is assumed to be much smaller in its third dimension (i.e. thickness) than its other two dimensions, and instead of specifying its thickness, the third dimension of the fracture is represented by a conductivity-thickness product, σt, determined by the average thickness of the fracture multiplied by the conductivity of the fluid in the fracture. This approach of defining a thin body via σt is standard for other EM imaging problems, for example, present day commercial marine CSEM used in exploration.

Inherent in the approach of combining conductivity and thickness into a single variable is that a thin high conductivity body produces the same EM signal as a thicker lower conductivity body of the same σt product. A second, more subtle consequence is that a series of thin bodies, of thicknesses t_1, t_2, t_3, .. t_n produce the same EM signal as a body of total thickness $t_T = t_1 + t_2 + t_3 + .. t_n$ provided the final total thickness, t_T, is still thin compared to the other fracture dimensions. In the second quarter, we realized we could use the summation property inherent in the σt approximation to provide a direct estimate of t_T without first requiring an estimate of the number of fractures (i.e., n in the summation $t_T = \sum_n t_n$) produced in a given fracturing stage.

Our goal is to map the propagation of fluid used to induce the fractures. It does not matter whether the fluid produces entirely new fractures or produces fractures that connect existing fractures. The total fracture thickness is related to the average surface area of new fractures, $\langle A_{frac} \rangle$ and volume of hydrofracturing fluid used by, $\langle A_{frac} \rangle \sum_n t_n = V_{fluid}$. Thus $t_T = V_{fluid}/\langle A_{frac} \rangle$.

For a typical 300 ft fracture stage in the Marcellus, V_{fluid}. = 10,000 bbls = 1.5 x 10^6 l (liters). For a single 100 m x 200 m fracture the total thickness is therefore calculated to be t_T = 7.5 cm. Figure 1 shows plan views and side elevation views of tomographic fracture images (TFIs) produced by our collaborator Global Microseismic Services (GMS) for a commercial fracturing project in the Marcellus shale. TFIs provide a voxel by voxel image of where seismic energy was released during the fracturing process. Figure 1 shows two roughly parallel fractures of lateral extent 160 m and 140 m, and height 220 m and 215 m corresponding to a total fracture thickness of 2.3 cm, or an average thickness of 1.15 cm per fracture. However it should be noted that the voxels in Figure 1 are 8 m (25 ft) cubes, and near to the casing, at least, there could be multiple fractures within each voxel, thereby reducing the thickness per fracture.

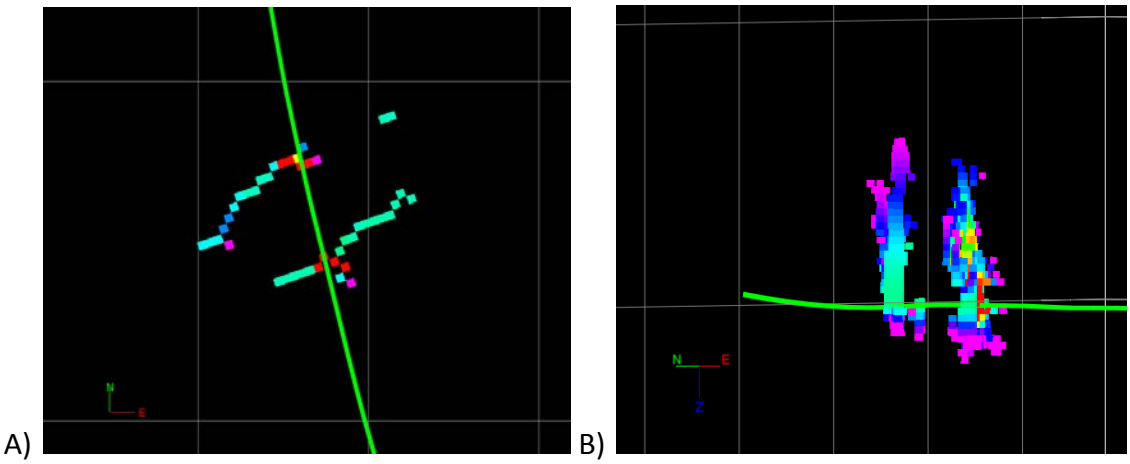

Figure 1. Typical tomographic fracture images for a commercial fracturing project in the Marcellus shale. A) Plan view. B) Side elevation. Individual image voxels are 8 m x 8 m x 8 m.

4.3.1.2 Task 2.1 Results

The goal of Task 2.1 is to relate the fractures to a change in electrical resistivity that can be used to project the electric field produced by the fracture at the surface. Brine of salinity 100,000 ppm has a conductivity at 50 °C of 20 S/m. Thus when modeling fracs of area 20,000 m^2 with 10,000 bbls of injected fluid, a σt value of 1.5 S should be used. If the models are run for a fracture size of 100 m x 100 m and the same volume of fracture fluid injected, a σt value of 3

should be used. Furthermore we have shown that fracture dimensions of 100 m x 200 m are appropriate for the Marcellus, and likely other shales of interest.

Task 2.1 is complete

4.3.1.3 Task 2.2 Calculate surface EM signal

Historically, the presence of conducting casings in boreholes has been considered a problem for traditional EM surveys (for which all equipment is deployed at the ground surface), and such surveys have been arranged to avoid placing sources or receivers close to casings. For the recently introduced borehole to surface EM (BSEM) method, the majority of commercial surveys have been conducted in uncased wells, thereby eliminating the question of current flow in the casing. However, the great majority of boreholes are completed with electrically conducting casing.

The standard method to model surveys and invert the measured data to illuminate the subsurface resistivity structure is to divide the volume of interest into many subvolumes (voxels) and solve for the EM fields at the boundaries of each voxel. A considerable practical challenge in using voxel based methods is to limit the total number of voxels while being able represent effects occurring over small length scales. For example modeling a region of extent 5 km x 5 km x 2 km with voxels of 10 m requires 50 million voxels, but is unable to represent features that vary on scales smaller than 10 m.

However, a casing of typical thickness is approximately 1 cm, much smaller than the smallest voxel used in a conventional EM model of the subsurface. One way to try to address this disparity in length scales between the dimension of a casing (1 cm) and the scale of the subsurface model 500,000 cm is to vary the voxel size so that it is smaller within in the casing and in the region around the casing and larger elsewhere. This approach of course increases the number of voxels required. Dividing a 10 m radius volume around a 2000 m long casing into 1 cm voxels adds approximately 6 billion voxels to the subsurface model. A further challenge is that the current density in the casing is still 1 million to 1 billion times higher than in the earth no matter how big the voxels are made.

To address this fundamental calculation problem GroundMetrics has devised a two step approach. First, to model the effect of a casing we make the approximation that because of the large conductivity difference between natural formations within the earth and the conductivity of a casing, the secondary field produced by an anomaly at distance from a casing produces a negligible effect on the current distribution in the casing. This approximation is equivalent to saying the primary field produced by a casing at a resistivity anomaly within the earth does not depend on the nature of that anomaly. Thus, the first step is to model the interaction of the casing with a layer earth to calculate the current distribution along the casing as a function of depth. Because no subsurface anomaly is present the casing can be modeled in an axially symmetric (i.e. 2D) coordinate system.

Secondly, once we have the current distribution along the casing we can represent that current via a series of current dipoles source and remove the casing itself from the model. Specifically, the region of the model where the casing is present in reality is rendered as a region of the natural formation that would be there in the absence of the borehole and casing, but containing a series of current dipoles oriented along the axis of the casing that are equal in magnitude to the current that was present in the casing, as illustrated in Figure 2.

For the first step, the current in the casing is modeled using the mathematical approach of Schenkel and Morrison.[2] This approach uses the surface integral equation (SIE) method and finds the potential on the surface of the scattering bodies. It can be used to simulate a casing and annuli in a layer medium. However, as shown in Figure 3, the SIE method produces a dip in current at the top of the casing that depends on the size of the mesh. An alternative approach is the volume integral equation (VIE) method.[3] It uses a thin sheet approximation and calculates the E-fields within an axisymmetric high conductive, longitudinally thin scattering body (i.e., the casing). However, this method only works in a uniform half-space (i.e., with no layers). The VIE solution is plotted in Figure 3 also to show how the SIE approach used in the program asymptotically converges on the correct current distribution.

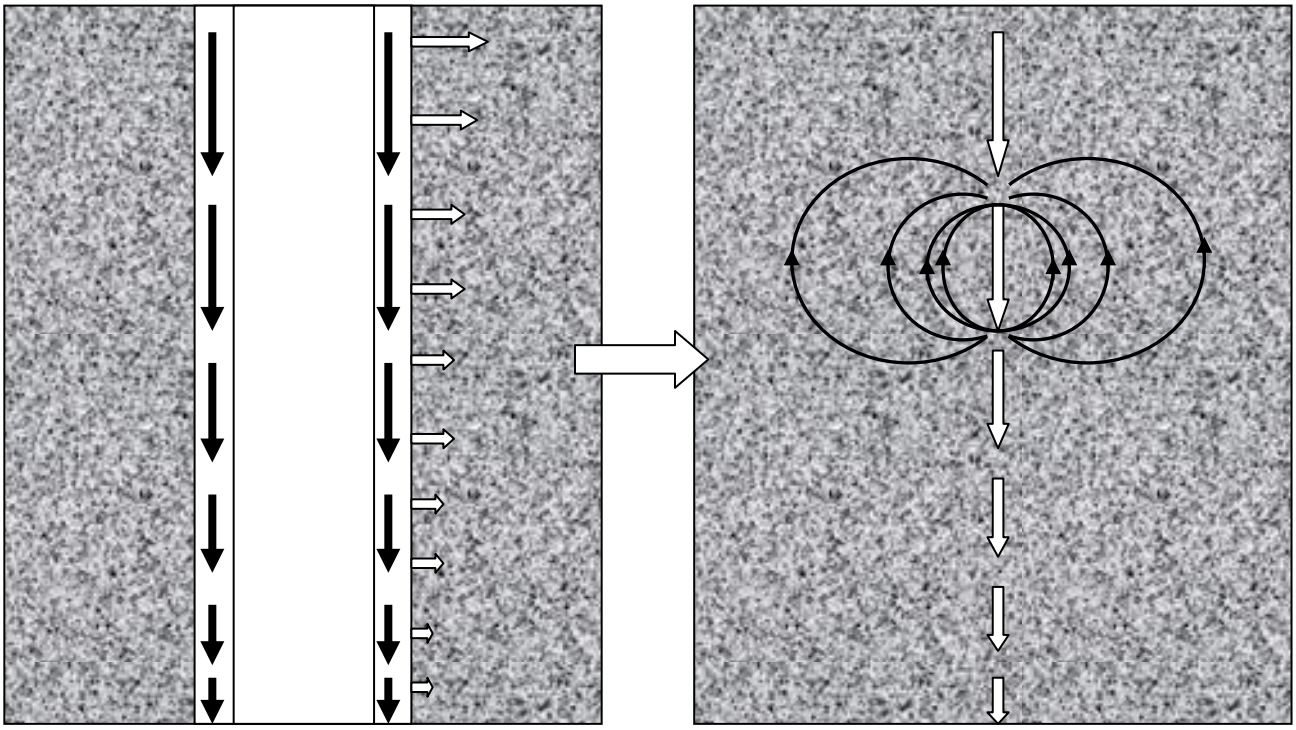

Figure 2. Representation of a conducting casing carrying an electric current (left) as a series of equivalent current dipoles in the host medium (right). The current in the casing is shown by the black arrows and varies along the length of the casing due to current flow from the casing into the medium which is illustrated by white horizontal arrows. In the right figure, the current flowing in the medium for one of the equivalent dipoles is illustrated by the black curved lines.

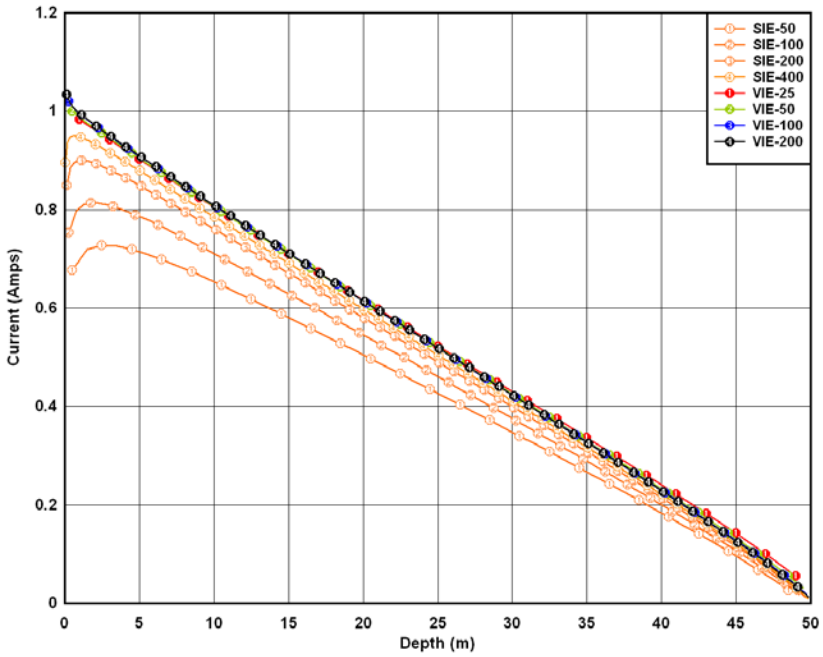

Figure 3. Current distribution along a casing in a uniform resistive medium as a function of the number of uniform mesh subdivisions along the casing length. The surface integral (SIE) method is used in this project, but has a dip in current at the top of the casing that depends on the size of the mesh. The volume integral equation (VIE) method is shown for comparison.

To the best of our knowledge there are no casing current solutions in the literature for the source configuration to be used in this program. Accordingly, to confirm the accuracy of our solution it was necessary to model a casing problem for which there are published solutions. One such configuration of significant practical interest is the split casing configuration shown in Figure 4A used to send electrical signals from the bottom of a well to the surface. Figure 4B shows a comparison of the GroundMetrics approach to calculating the current distribution for a split casing with a published solution by DeGauque.[4] The two results are very similar, but near to the top of the casing the current calculated by the GroundMetrics approach is smaller. Figure 5 shows a second comparison, this time with a more recent solution for the same problem by Trofimenkoff.[5] The agreement is very good.

A)

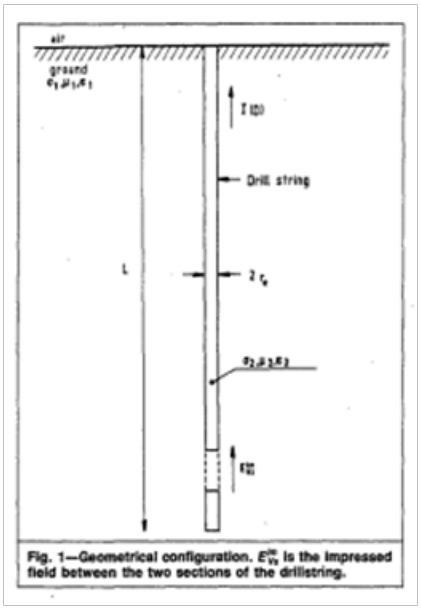

B)

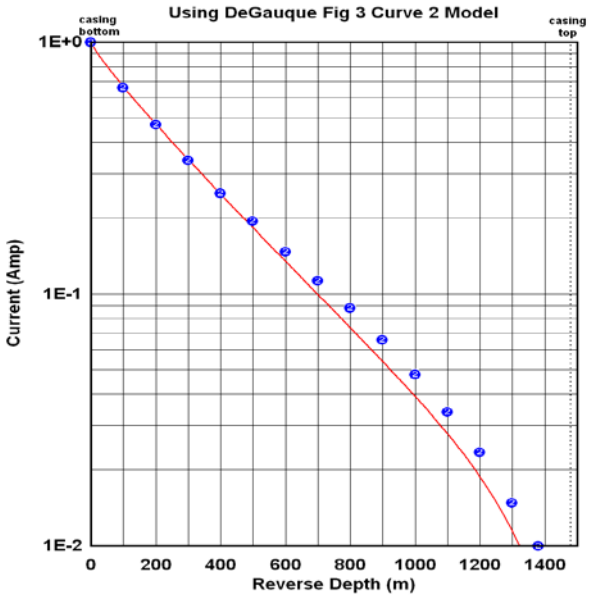

Figure 4. Comparison for solutions for a casing driven as a split dipole. A) Split casing source geometry. B) Calculated current along the casing. Red line: GroundMetrics. Blue symbols DeGauque solution

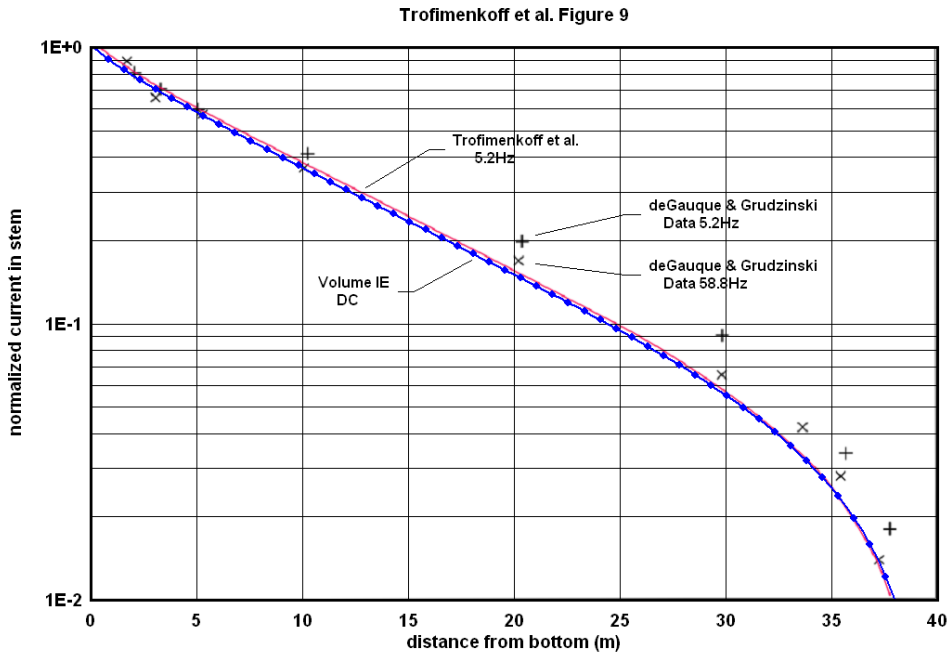

Figure 5. Second comparison of solutions for a casing driven as a split dipole

To implement the second step of our approach, the casing current solution is used as an input to a complete 3D electromagnetic (i.e., AC) code. As discussed in the previous report, we decided to modify a code developed by Drs. Frank Morrison and J. Torquil Smith[6,7] by enabling the code to include an array of subsurface current dipoles.

4.3.1.4 Task 2.2 Results

The modified 3DEM code has been completed. A comparison of the surface E-field calculated for a layered earth by the new 3DEM code and the prior 2D casing code is shown in Figure 6. The mesh used in the two models is different, and considering this different the agreement between the two models is adequate. We are in the process of expanding our computer system to enable a finer mesh in the 3D code, comparable to that in the casing 2D code.

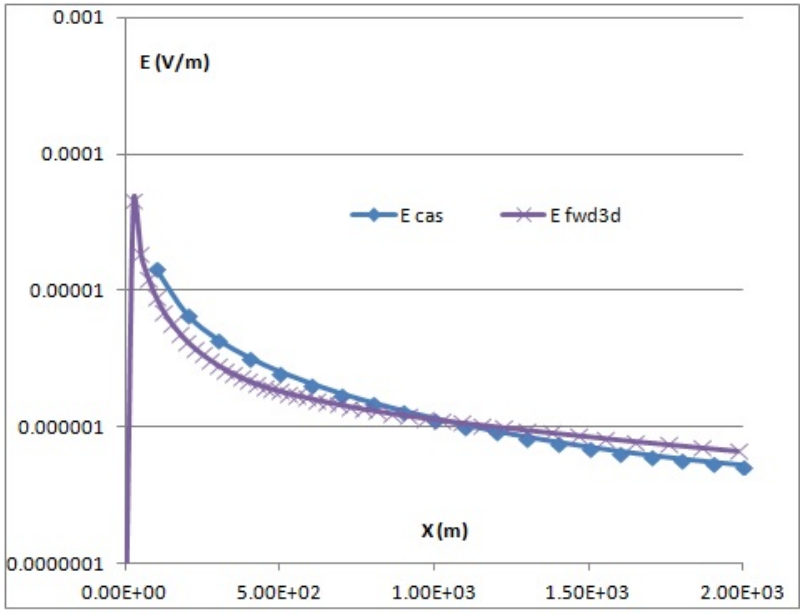

Figure 6. Surface E-field as a function of lateral distance from a casing in a layered earth model. Blue: 2D casing code. Purple: new 3DEM solution

The 3DEM code allows us to calculate the signature of a hydrofracture produced by current flow along a true 3D casing comprising a horizontal section connected to a vertical section and

located in a layered earth. Figure 8 shows the change in the lateral position of the peak in the surface electric field due to a fracture near to a horizontal section of a casing vs. the actual position of the fracture along the horizontal section. We see that the peak in fracture signal moves in physical correlation with the location of the fracture.

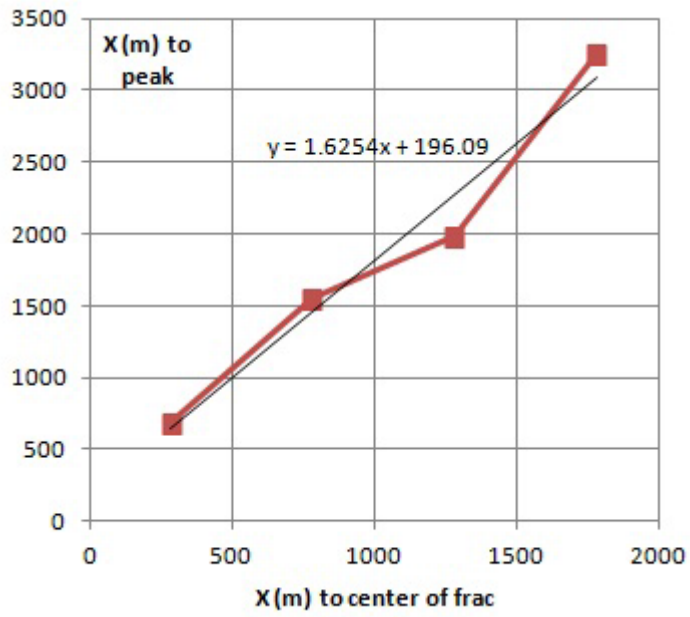

Figure 7. Results of 3DEM modeling of a 60 m x 200 m fracture near to a horizontal section of a casing. Vertical axis: lateral position of the peak in the surface electric field due to the fracture. Horizontal axis: the actual position of the fracture along the horizontal section

The percentage variation in the surface fracture signal as a function of fracture width is shown in Figure 8. Again the surface signal behaves in a physically reasonable manner.

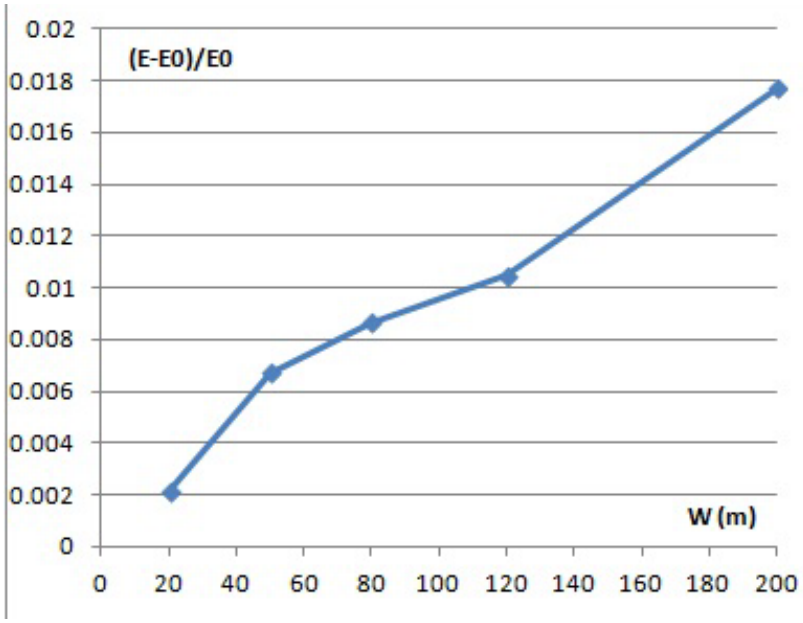

Figure 8. Percentage change in the surface electric field as a function of the width of a hydrofracture adjacent to the horizontal section of a directionally drilled well

With these results we have completed program milestone 1: *Completion of Code to Calculate the DSEM Signal for a Horizontal Well.* The verification method for this milestone is described in the project management plan as follows:

Verification Method: Review of the outcome of multiple runs of the calculation to confirm: a) the projected signal is reasonable when compared to resistivity solutions for a vertical well with similar background bulk conductivity, b) the calculation scales in a physically realistic way with depth and offset from the well, and c) the calculation converges to a similar solution for different but similar starting points to confirm the solutions are not metastable.

4.3.2 Task 3 – Expand Survey Capability for Simultaneous Monitoring

A hydrofracking stage involves a series of unique events particular to the host geology that cannot be repeated and reproduced. Thus, all sensors must be in place and running in advance of the fracking process. At the time the project began, GroundMetrics had the capability to deploy up to 10 data recorders. To deploy a substantially larger number it is necessary to be

able to monitor each sensor channel from central locations. Effort has been conducted towards this goal as detailed in the following.

A test was recently conducted at Ocotillo Wells CA as part of our IR&D effort that is relevant to this project. A survey map is shown below.

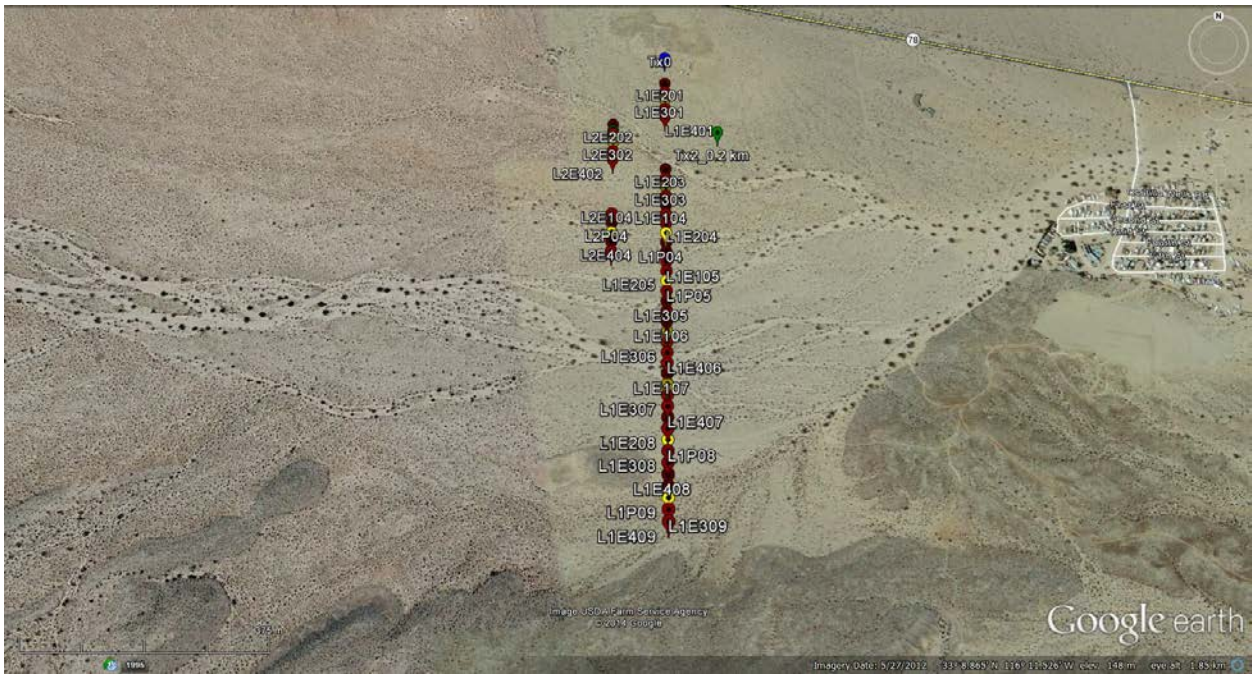

Figure 9. Map showing survey layout

During this effort, we tested three system components:

4.3.2.1 Real-time quality control software

The real-time quality control software is used to remotely monitor data from deployed Eos systems from a central location in near real time. Before we developed this software, the deployment team had to check each system individually to confirm it was deployed correctly (sensors connected to the correct ports, ground stake in good contact with the ground, etc.) using a different piece of software. They were unable to check noise, and the only way one could determine if a system had been disturbed after deployment was to physically check on the system at its location. In general, if a system was disturbed after it was deployed, this fact was not discovered until someone went to move the system to its next location. If the system

had been disturbed, data were often nonexistent or unusable, then systems had to be left in place after reinstallation to collect necessary data, extending the survey duration.

The real-time QC software allows one person, the observer, to monitor all deployed systems to confirm they have been deployed correctly, monitor source transmit cycles, and ensure the systems have not been disturbed. This helps speed up the deployments, and instead of needing one person per deployment team that can debug a system, having 1-2 people per survey that can debug a system is adequate. This means we need fewer workers for deployments, and surveys can be kept on schedule more efficiently.

The real-time quality control software processes 5-minute chunks of downloaded data. It summarizes the results of the processing in a table (see Figure 10). Any time there may be a problem with the deployment, the text changes to red so the observer knows to check that system. The red values may or may not be in line with expectations for that system depending on its setup and the survey conditions. If the observer needs more information about a particular system, a layout can be created from the table. The layout will show magnitude, noise and coherence in the Fourier domain as well as filtered and unfiltered time domain data so the observer can see exactly what that system recorded during the most recent 5-minute period and assess whether a re-installation might be required.

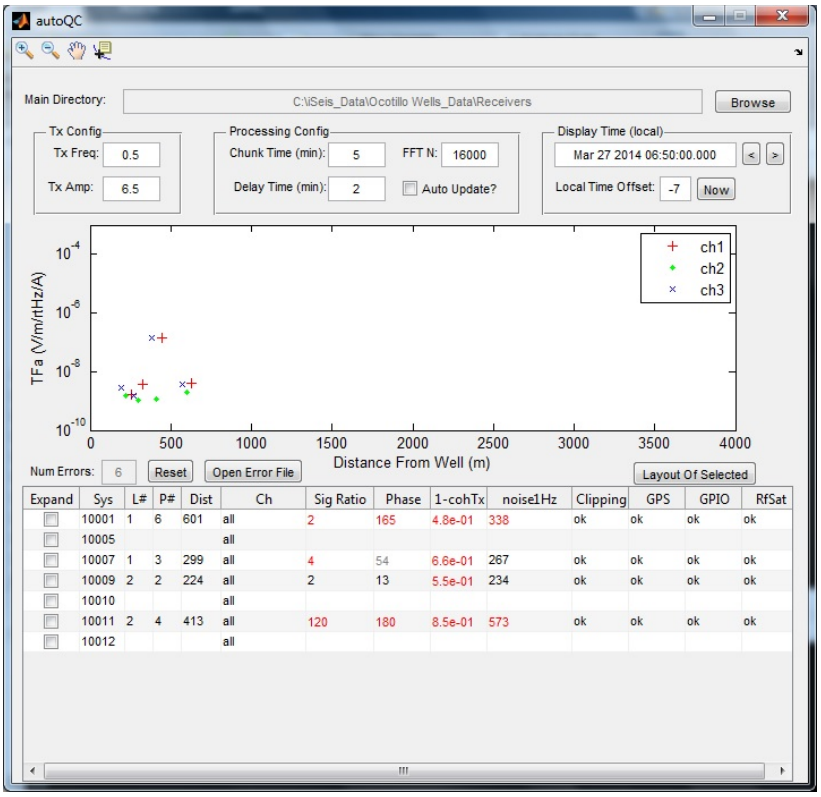

Figure 10. Real-time QC software screenshot

4.3.2.2 Eos control software (used at base station to communicate with all Eos data acquisition units)

The Eos control software is made up of 2 main pieces of software - Sigma Observer and Data Collector. Sigma Observer can be used to sleep/wake the Eos and enable/disable the Wi-Fi (both functions are used to extend battery life). It is also used to monitor the battery life and GPS. Sigma Observer controls the Data Collector program, which is used to remotely download (over Wi-Fi antennas) data from the Eos systems in near real time.

A few modifications were made to the software so it would work better for our application. The Eos records data on 3 channels. Channels 1 and 3 are fixed. They always record data from specific input ports. Channel 2 is variable. The software and firmware were modified so that a specific dipole is recorded on Channel 2 by default, but we can change what is recorded on Channel 2 through the Sigma Observer program. This is occasionally used to troubleshoot

deployments in the field. A modification was also done to the Data Collector program to allow us to download 15-second files (the file length we use) automatically.

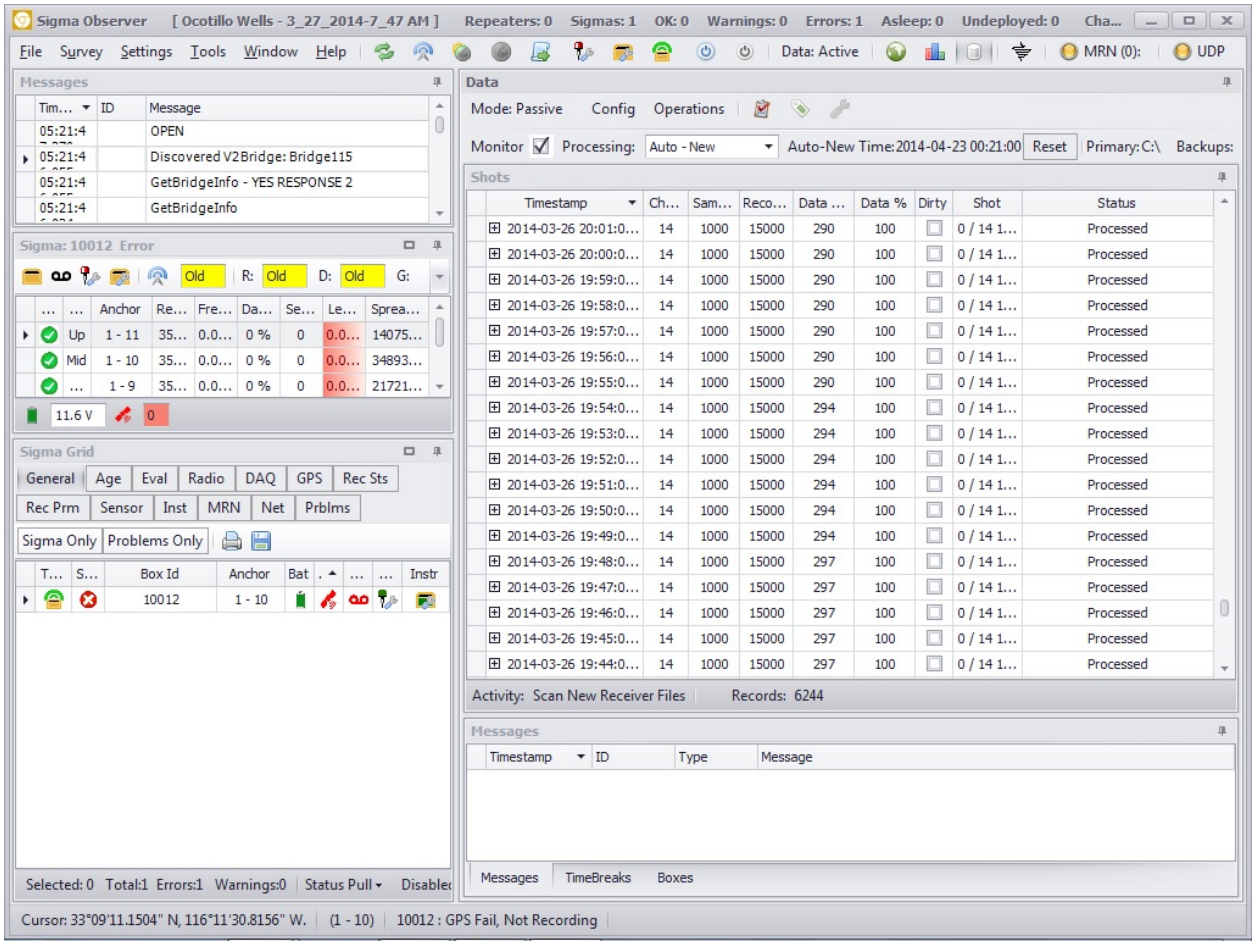

Figure 11. Sigma Observer Screenshot

The tests went well and the new capabilities are functioning as desired.

4.3.2.3 New GPS system.

GroundMetrics is evaluating the Trimble GeoExplorer XH 6000 GPS system which has specifications that indicate it can provide accuracy adequate for our application at a reduced price.

GroundMetrics has been using Real Time Kinematic (RTK) positioning units in its surveys and these have functioned well, but their high price limits their practicality for large surveys

requiring multiple units. Our research had suggested that other Trimble units with slightly less precision but at a much lower price point might be adequate for our needs, so we did an investigation of the Trimble GeoExplorer XH 6000 while we were conducting our latest test.

Figure 12. Trimble GeoExplorer XH 6000

A GeoExplorer unit with external Tornado antenna was rented for the Ocotillo Wells trip in order to evaluate its accuracy and ease of use. It was used in three different scenarios:

1) Accuracy test – points were measured at known distances apart. Then data were post-processed and distances calculated to confirm the distances were correct to within the accuracy of the device.

2) Sensor and DAQ positions were surveyed in using a Garmin GPS. Then the positions were recorded with the XH 6000. The Garmin is accurate to within a few meters so it was expected that the actual dipole lengths to be within a few meters of the planned dipole lengths.

3) Sensor and DAQ positions were surveyed in using the XH 6000. The field accuracy of the device is submeter so it was expected that the actual dipole lengths to be within 1 meter of the planned dipole lengths.

Summary of Test 1 – Accuracy test

Four points were recorded. Points 1 and 2 were 168 cm apart, and points 3 and 4 were 200 cm apart. These distances were measured with a tape measure, and then the recorded data were post-processed to apply differential corrections from a reference station. The distance between the corrected points was calculated. The following table summarizes the results.

	Actual Distance	**Calculated Distance**	**Error**
Point 2 – Point 1	168 cm	170.8 cm	2.8 cm
Point 3 – Point 4	200 cm	199.7 cm	0.3 cm

As one can see from the table, the differences between the actual distances apart and the calculated distances apart are well within 10 cm, which is the advertised accuracy of the device.

Summary of Test 2

All points for L1P03 and L1P05 as well as L2E104 were surveyed in with a Garmin RTK system as a baseline, and later the points were recorded with the XH 6000. From the following table one can see that the dipole lengths are all within 3 m of the planned dipole lengths, as expected. Note that for L2P04 there were only 2 sensors (1 dipole) connected. The sensors were placed at L2E104 and L2E404 so they were 80 meters apart. They were connected to port 2 and port 3, respectively, so that CH 3 recorded data from L2E104, and CH 1 recorded data from L2E404.

Dipole	**Planned Dipole Length (m)**	**Measured Dipole Length (m)**	**Difference (m)**
L1P03 – CH 1	20	22.486	2.486
L1P03 – CH 2	40	39.462	0.538

L1P03 – CH 3	20	20.652	0.652
L1P05 – CH 1	20	17.412	2.588
L1P05 – CH 2	40	42.565	2.565
L1P05 – CH 3	20	19.259	0.741
L2P04 – CH 2	80	82.780	2.78
L2P04 – CH 3	40	42.612	2.612

Summary of Test 3

All points for L1P06 and L2P02 as well as L2E404 were surveyed in with the XH 6000. From the following table one can see that the actual dipole lengths are all within 1 m of the planned dipole lengths, which is what we would expect since the field accuracy of the XH 6000 is submeter.

Dipole	**Planned Dipole Length (m)**	**Measured Dipole Length (m)**	**Difference (m)**
L1P06 – CH 1	20	20.224	0.224
L1P06 – CH 2	40	39.663	0.337
L1P06 – CH 3	20	20.169	0.169
L2P02 – CH 1	20	19.947	0.053
L2P02 – CH 2	40	40.579	0.579
L2P02 – CH 3	20	19.783	0.217
L2P04 – CH 1	40	40.236	0.236

Results and Conclusions

The XH 6000 performed as expected with submeter field accuracy and decimeter post-processed accuracy. Surveying speed and accuracy might improve with the use of a range pole.

Additionally, field crews assessed that there may be a way to improve post-processed accuracy to the centimeter level with a software (and maybe a hardware) upgrade to the XH 6000. Also, field accuracy can be improved to the decimeter level (maybe centimeter level with the hardware and software upgrades) with the use of VRS (Virtual Reference Station) technology, which provides real-time corrections from reference stations.

4.3.2.4 Additional EOS build

15 kits were built, each kit = 1 Eos and 4 eQubes. There were 2 substantial improvements made to this version of the Eos from our base unit.

1. VHF radio capability. Timing of data acquisition is crucial information for processing. Our Eos units establish time through GPS services. However, in dense tree canopies, GPS access can sometimes be difficult to maintain. With the new capability, any unit that senses an absence of GPS connection will automatically link to its master unit by VHF radio. This gives us the freedom to place our Eos units where needed with only the master unit needing a deployment location free of possible GPS interference overhead.

2. Higher quality precision voltage reference for the Analog-to-Digital Converter (ADC). The previous chip offered accuracy with a .1% variance of signal amplitude. Our sophisticated approach to this project's scientific problem would benefit from improved accuracy and thus we upgraded to a chip with .05% variance specs. In addition, the new chip offers substantially (62%) better temperature stability, important for an outdoor application in various types of weather.

Figure 13. New Eos data acquisition units

4.3.2.5 Additional eQube build

GroundMetrics increased its sensor inventory substantially with a build of many units of the latest version of the device. This model features a refined circuit design that improves its sensitivity, a new form factor that makes it easier to hold and place, improved manufacturability, and a color chosen for improved visibility. Figure 14 shows an older eQube next to the latest version.

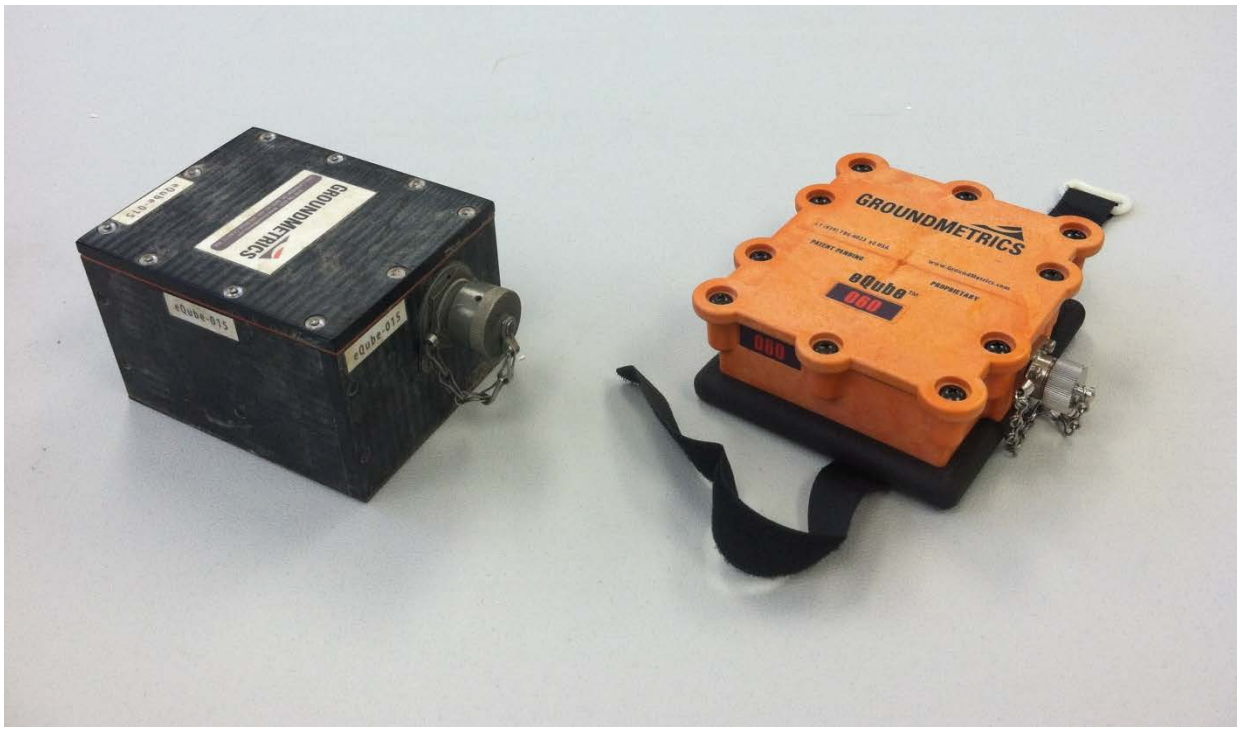

Figure 14. Old (left) and new (right) version of GroundMetrics e-field sensors

These builds fulfill Milestone 2, Assembly of the DSEM Sensor and Receiver Hardware. The verification method listed in the project plan is as follows and has been carried out: Laboratory calibration of all sensor and receiver channels to confirm operation against documented specifications.

4.3.3 Task 5.0 - Quantify the Resistivity Change Produced by Hydrofracturing

The goal of Task 5 is to process the data collected in Task 4 to identify an EM signal unequivocally related to hydrofracturing in the expected region.

4.3.3.1 Subtask 5.1 Process DSEM Data to Extract the EM Signal Change Due to Fracking

In the first quarterly report we showed an improvement in the detectability of the smallest detectable signal from 10^{-10} V/m to 10^{-11} V/m by stacking DSEM data over its collection interval to increase signal-to-noise ratio. We have begun to write codes to do this stacking automatically, and we intend to further test this approach in the third quarter.

4.3.3.2 Subtask 5.2 Develop 3D DC Inversion of the EM Data

Our initial results indicate that the AC response of a fracture can include important information and we have first investigated broadening Task 5.2 to include a complete EM inversion, i.e. including frequency dependent information. The industry standard code for doing a 2DEM inversion is the MARE2DEM code developed by the Seabed Electromagnetic Methods Consortium (SEMC) at the Scripps Institute of Oceanography (SIO) in San Diego. By good fortune this code was released for free public access on January 1, 2014. A two dimensional code can be used to invert 3D real world data provided the data are acquired in planes that intersect the (3D) target approximately symmetrically. This is the approach taken by the marine EM survey companies EMGS and PGS, both of whom use MARE2DEM for commercial projects. Given that a fracture is approximately centered on the horizontal section of the casing, we can arrange the EM survey to exploit this symmetry.

However, neither the SIO code, and indeed nor any other prior EM code, can presently mathematically represent a well casing for the reasons discussed in Task 2. Further the MARE code can only accommodate a single EM source. After meeting with the senior developers of the MARE2DEM code, we have defined a series of modifications to enable it to input a series of current dipoles in accordance with the casing representation described in Task 2.

4.3.3.3 Presentations

We have submitted abstracts to and been accepted for presentations at the Society of Petroleum Engineers' Annual Technical Conference and Exhibition (SPE ATCE), the European Association of Geoscientists and Engineers' (EAGE) 76th Annual Conference, the SEG/SPE/AAPG/SPWLA/AEGE Summer Research Workshop, and the SEG 2014 Development and Production Forum meeting "Reservoir Characterization and Monitoring with Advanced Geophysical Technology."

These presentations will be at least partially related to this project and the DOE will be acknowledged. Once the presentations/papers are complete, they will be submitted to the DOE.

4.3.4 Next Reporting Period

There are no milestones scheduled for the next reporting period, but we will continue finalization of the code, fine-tuning of models and definition of the survey plan in the next quarter. Mobilization and logistics work will also begin.

5 Products

There are no completed products for this project after only two quarters of performance. Working with collaborator Berkeley Geophysics Associates, we have completed a preliminary calculation of the signal produced by a hydrofracture using an adaptation of a prior published model.[8] Once this model has been validated, it will be considered a product of this project, but considerable validation will be needed before the model and its outputs will be deemed ready for publication.

6 Participants & Other Collaborating Organizations

6.1 GroundMetrics, Inc.

GroundMetrics is leading the project as well as developing the project hardware for the EM measurements. Our staff is led by Dr. Andrew Hibbs, project PI. We have a number of engineers in our 2 and 1 labor categories, and only 3 of them worked more than a man-month on this project this reporting period as the work spread across the staff.

Name:	**Dr. Andrew Hibbs**
Project Role:	PI
Nearest Person Month Worked	1
Contribution to Project:	Dr. Hibbs is overseeing the technical work, particularly the development of the computer code.
Funding Support	N/A
Individual in Foreign Country	N/A
Travelled to Foreign Countries	N/A

Name:	**Ms. Stacy Kouba**
Project Role:	Staff Scientist Level 2
Nearest Person Month Worked	2.5
Contribution to Project:	Ms. Kouba led specifications for, and build coordination and acceptance testing of our hardware, as well as participation in field testing.

Funding Support	N/A
Individual in Foreign Country	N/A
Travelled to Foreign Countries	N/A

Name:	**Mr. Joseph Pendleton**
Project Role:	Engineer Level 2
Nearest Person Month Worked	2
Contribution to Project:	Mr. Pendleton worked on building and testing equipment.
Funding Support	N/A
Individual in Foreign Country	N/A
Travelled to Foreign Countries	N/A

Name:	**Mr. Edward Molder**
Project Role:	Engineer Level 1
Nearest Person Month Worked	1
Contribution to Project:	Mr. Molder worked on building and testing equipment, particularly field testing.
Funding Support	N/A
Individual in Foreign Country	N/A
Travelled to Foreign Countries	N/A

During this reporting period, Chief Engineer Todor Petrov left GroundMetrics. His work on this project is going to be handled by a combination of new employees, increased hours for Dr. Hibbs, increased consulting allocation and the addition of a Chief Geophysicist, a position we plan to fill by June.

GroundMetrics has added an Executive VP of Operations who will be taking over logistics and will assume that side of Mr. Petrov's function. This comprises supervision of equipment preparation for deployment, assignment of personnel, and calendaring. Dr. Hibbs' role has been expanded to cover some of the scientific side of Mr. Petrov's original allocation and we have also added consultant Dr. Daniel Lathrop, who will be responsible for high-level coding and processing.

6.2 Berkeley Geophysics Associates

Our subcontractor Berkeley Geophysics Associates is currently working with us on the calculation of a signal produced by a hydrofracture. BGA is headquartered in Berkeley, CA and led by Prof. Frank Morrison of the University of California, Berkeley.

6.3 Global Microseismic Services

Our subcontractor GMS is providing seismic services to the project. GMS's main contribution will come when we do our large data collection, but in the previous reporting period they provided us with TFI information to incorporate into our modeling and calculations. This necessitated a shift of funds from their Year 2 to their Year 1 allocation.

7 Impact

As the project has only completed two quarters of work, there is not yet any impact to describe specifically from those two quarters. However, the potential impact of the overall project could be substantial.

Fracking is more expensive than conventional methods used to produce gas and oil, and fracked wells exhibit a much faster decline in production than conventional wells. Furthermore there are environmental concerns with the amount of water that is needed, pollution of groundwater reservoirs, and earthquakes caused by hydrofracturing or water disposal. This program may offer a methodology that can achieve complex mapping of subsurface fluids to monitor the fracking process.

Knowledge of fracture networks can be used to define frac stage locations and the duration of pumping at each stage. Tomographic Fracture Imaging™ is a proprietary technology of project team member Global Microseismic Services' (GMS) parent company Global Geophysical Services, Inc. (GGS) that produces a 3D image of the natural fracture network in the Earth. Seismic emissions of much smaller magnitude than are detectable by hypocenter methods are extracted from the trace data. However, while TFI produces images of entire fracture networks, the underlying data represent the fracture of the host rock, not the passage of fluid into the new pore spaces and the resulting increase in porosity.

The addition of a resistivity image, the innovation being pursued under this project, will provide an independent image of the change in fluid distribution in the ground. Such fluid imaging is a basic capability that tracks the core physical property that fracking is designed to change, and may enable new capabilities such as measurement of tensile fractures (instead of only shear).

Accurate monitoring of SRV is the key to improving not only the operational efficiency of hydrofracturing but also confidence regarding fluid propagation and fracture trajectory below ground during fracking. Operationally, the potential exists to monitor the change in rock porosity resulting from each frac stage. Accordingly there are a wide range of potential benefits, including:

A. Reduced cost and use of fracture fluid by reducing the number of fracture stages.

B. Improved recovery and reduced environmental impact via improved mapping of fracture propagation.

C. Reduced cost from replacing high cost aspects of a microseismic seismic survey with EM elements. Extension of microseismic methods to formations where they currently are problematic and provide inadequate information.

D. Developing & demonstrating ways to monitor hydrofrac height growth,

For the completion engineer, improved information directly affects the four major decisions about the well: stage spacing (# and distance between fracs), stage volume (fluid and proppant), stage rate, and fluid viscosity. For developmental geologists, the improved knowledge will indicate how far the proppant fluid is being placed. For regulatory agencies, tracking fluid movement and quantity will provide valuable information to make project decisions.

Economic benefits to the public include reduced energy costs, reduced reliance on foreign sources of energy, and increased domestic economic activity. Potential environmental advantages include reducing the amount of water used in fracking, reducing the activity at fracking sites resulting in reduced traffic, noise and associated surface contamination, and providing physical monitoring for projects that cause environmental concerns.

8 Conclusion

The project is moving along well. We have confirmed our 3D code is running correctly, and completed some preliminary signal modeling. We have completed modifications to our Eos and eQube units and the new devices have been delivered to GroundMetrics' offices, where acceptance and characterization testing is underway. We have been accepted to present at multiple conferences, including SPE and EAGE's large annual meetings.

9 Acknowledgment

This material is based upon work supported by the Department of Energy under Award Number DE-FE0013902.

10 Plans for Next Reporting Period

The program is on schedule and we expect tasks will be addressed and completed as per the program management plan. For convenience, the major tasks for the third quarter are as follows:

- Continue testing and improving code function
- Final site verification
- Survey plan

11 Milestones Not Met

None.

12 Cost Status

Budgeted	Year I		Year 2			Actuals - Fed only		
Budget	Federal	Non Federal	Federal	Non Federal	Total	10/13-12/13	1/14/-3/14	Total
Salaries	267,110	25,960	51,715		344,785	$ 58,698	$ 83,243	$141,941
Travel	10,267		867		11,134	$ 1,155	$ -	$ 1,155
Consultant Services	42,500				42,500	$ 13,688	$ 6,531	$ 20,219
Materials	183,900				183,900	$ -	$ 34,920	$ 34,920
Equipment	20,121	9,371			29,492	$ -	$ -	$ -
Subcontracts	535,000		305,000		840,000	$ -	$ -	$ -
ODC	570	501			1,071	$ -	$ -	$ -
Direct Costs	1,059,468	35,832	357,582		1,452,882	$ 73,541	$124,695	$198,235
Indirect Costs	576,598	41,835	133,359		751,792	$146,728	$204,072	$350,799
Other		583,333			583,333	$ -		$ -
Total	1,636,066	661,000	490,941		2,788,007	$220,268	$328,766	$549,034

The budgeted items reflect our current project management budget, and a modification request is in process.

References

[1] Dey, A. Morrison, HF. Resistivity Modeling for Arbitrarily Shaped Two-Dimensional Structures. Geophysical Prospecting Volume 27, Issue 1, pages 106–136, March 1979

[2] Schenkel, C. J. and Morrison, H. F., 1994, Electrical resistivity measurement through metal casing: Geophysics, 59, no. 7, 1072-1082.

[3] Schenkel, C.J., Morrison, H.F. Effects of well casing on potential field measurements using downhole current sources. Geophysical Prospecting, Vol 38, No 6, August 1990. pp. 663 - 686

[4] DeGauque, P., Grudzinski, R., Propagation of Electromagnetic Waves Along a Drillstring of Finite Conductivity. SPE Drilling Engineering, June 1987.

[5] Trofimenkoff, F.N, Segal, M., Klassen, A., Haslett, J. W.., Characterization of EM downhole-to-surface communication links. IEEE Trans. on Geoscience & Remote Sensing. Nov. 2000.

[6] Smith, J.T., Conservative modeling of 3-D electromagnetic fields, Part l: Properties and error analysis. Geophysics, 61: 5, Sept-Oct 1996.

[7] Smith, J.T., Conservative modeling of 3-D electromagnetic fields, Part ll: Properties and error analysis. Geophysics, 61: 5, Sept-Oct 1996.

[8] Dey, A. Morrison, HF. Resistivity Modeling for Arbitrarily Shaped Two-Dimensional Structures. Geophysical Prospecting Volume 27, Issue 1, pages 106–136, March 1979